

# Effects of Glass Texturing Structure on the Module Efficiency of Heterojunction Silicon Solar Cells

Hyeongsik Park<sup>1)</sup> · Yoo Jeong Lee<sup>2)</sup> · Myunghun Shin<sup>2)\*</sup> · Youn-Jung Lee<sup>1)</sup> · Jaesung Lee<sup>2)</sup> · Changkyun Park<sup>3)</sup> · Junsin Yi<sup>1)\*</sup>

<sup>1)</sup>College of Information and Communication Engineering, Sungkyunkwan University (SKKU) Suwon, Gyeonggi, 16419, Korea

<sup>2)</sup>School of Electronics, Telecommunications and Computer Engineering, #76, Korea Aerospace University (KAU), Goyang, Gyeonggi, 10540, Korea

<sup>3)</sup>Crystalline Part, JUSUNG Engineering Co. Ltd., Opo-ro, Gwangju-si, Gyeonggi, 12773, Korea

Received September 18, 2018; Revised October 15, 2018; Accepted October 15, 2018

**ABSTRACT:** A glass-texturing technique was developed for photovoltaic (PV) module cover glass; periodic honeycomb textures were formed by using a conventional lithography technique and diluted hydrogen fluoride etching solutions. The etching conditions were optimized for three different types of textured structures. In contrast to a flat glass substrate, the textured glasses were structured with etched average surface angles of 31–57°, and large aspect ratios of 0.17–0.47; by using a finite difference time-domain simulation, we show that these textured surfaces increase the amount of scattered light and reduce reflectance on the glass surface. In addition, the optical transmittance of the textured glass was markedly improved by up to 95% for wavelengths ranging from 400 to 1100 nm. Furthermore, applying the textured structures to the cover glass of the PV module with heterojunction with intrinsic thin-layer crystalline silicon solar cells resulted in improvements in the short-circuit current density and module efficiency from 39 to 40.2 mA/cm<sup>2</sup> and from 21.65% to 22.41%, respectively. Considering these results, the proposed method has the potential to further strengthen the industrial and technical competitiveness of crystalline silicon solar cells.

**Key words:** Honeycomb glass, Heterojunction with intrinsic thin-layer (HIT) solar cell, Current, Solar module

## 1. Introduction

To date, crystalline silicon (c-Si) solar cells have been widely employed in mainstream photovoltaic (PV) products in solar cell industry. In the research area, Si heterojunction intrinsic thin-layer (HIT) solar cells showed the highest recorded efficiency of 26.6% for c-Si solar cells<sup>1)</sup>. HIT solar cells have attracted considerable attention because of their simple structure, as it affords the advantage of low-cost manufacturing, which thus promotes high efficiency. HIT solar cells have thin hydrogenated amorphous silicon (a-Si:H) layers covering the anterior and posterior faces of a c-Si wafer, and is well known that these thin a-Si:H layers can reduce the recombination loss of light-generated carriers on the wafer surfaces, increase the open-circuit voltage ( $V_{OC}$ ), and reduce the temperature coefficient of the device<sup>2)</sup>.

Although HIT solar cells have demonstrated excellent performance as solar cells, many factors, including the following,

still need to be addressed before they can be effectively applied to PV modules: undesirably high temperature coefficient, irradiance degradation, soiling damage, spectral dependency, angular losses, electrical instability, and optical loss<sup>3,4)</sup>. Because the most significant loss in PV modules is optical loss, which occurs as a result of reflection on the anterior surface of the cover glass, reducing this reflection serves to directly increase the short-circuit current ( $I_{SC}$ ) of a module assembled with HIT solar cells.

Various approaches such as anti-reflective (AR) coatings with dielectric films, localized laser roughening, and surface texturing on the anterior surface of a cover glass have been implemented to reduce the optical loss. Although the AR effects can be simply realized via optical destructive interference, a broad interface reflectance reduction requires graded refractive index (RI) structures<sup>5)</sup>; graded RI structures such as nano-textured surfaces, a porous surface produced by sol-gel liquid processing, or nature-inspired moth's eyes<sup>6)</sup> can be implemented, but the complexity of these structures makes them expensive. Furthermore, the implementation of localized laser roughening can enable light scattering on the surface to reduce the internal

\*Corresponding author: junsin@skku.edu

reflection loss between the glass and cell, but it still promotes reflection of the cover glass of the module<sup>7-9</sup>). Conversely, texturing a glass surface can be employed as a cost-effective means of reducing the optical loss and trapping the incident light within the module to increase the  $I_{SC}$  of the module<sup>10,11</sup>). Moreover, texturing has the following effects: 1) an anti-reflection effect owing to the high angles of incidence, and 2) a light-gathering effect owing to the micro-lens structure.

Cover glass texturing can be achieved via a dry or wet etching process. Dry etching entails physical ion bombardment and plasma reactive ion etching (RIE) in a vacuum, whereas wet etching applies direct surface treatments to the glass using acid and base etching solutions<sup>12-14</sup>). In general, researchers have focused on developing a fabrication method for the PV module that implements a dry-etching inductively coupled plasma RIE process to achieve a surface with high root-mean-square (RMS) roughness and a high haze ratio<sup>15,16</sup>). However, because dry etching cannot be effectively applied to large-area cover glasses, there is a high manufacturing cost for commercialization. In a recent study, Zhang *et al.* applied chemical wet etching with photo-resist (PR) patterns to glass surfaces to realize a high-efficiency module<sup>17</sup>); they demonstrated that the surface morphology and haze ratio significantly affect light-scattering performance.

This study was purposed to optimize the textured structure of the cover glass of HIT PV modules, and to assess the resulting improvement in module efficiency. To realize these aims, we applied chemical texturing to the cover glasses of HIT Si solar cells and systematically analyzed the effects of texturing on the performance of the HIT Si modules. More specifically, we applied periodic honeycomb texturing to HIT Si cell cover glasses and investigated the resulting optical behaviors and effects on the electrical properties of the PV module.

## 2. Experimental details

We used a chemical etching method with photolithography to obtain a honeycomb-textured structure on glass substrates. The periodic texturing patterns were formed on the glass substrates by using a combined technique that includes wet chemical etching and a hard mask of photoresist/hexamethyldisilazane (PR/HMDS); the process is illustrated in Fig. 1(a). First, Corning Eagle XG glass was ultrasonically cleaned with acetone, isopropyl alcohol (IPA), and deionized water for 10 min. each. A basic photolithography process was used to form the hard mask

needed to create periodic patterns. A spin coater was used to apply the HMDS layer in sequential rotation steps (1<sup>st</sup> step: 1000 rpm, 5 s; 2<sup>nd</sup> step: 2000 rpm, 40 s; 3<sup>rd</sup> step: 1000 rpm, 5 s); the HMDS layer was then baked for 3 min. at 150°C to harden the HMDS. The PR (AZ GXR-601-46 cps) was also stacked in a similar manner by using the spin coater (1<sup>st</sup> step 1000 rpm, 5 s; 2<sup>nd</sup> step 5000 rpm, 20 s; 3<sup>rd</sup> step: 1000 rpm, 5 s) and baked in a dry oven (110°C, 10 min.). The periodic pattern (opened circular holes: 3 μm in size with a 6-μm period) was then applied to the PR/HMDS by using ultraviolet photolithography before being baked for 15 min. at 140°C. The glass-texturing chemical-etching technique was performed in a circulating wet etching chamber in which the initial etching temperature was maintained throughout the etching process. The glass substrates with the PR/HMDS masks were etched in diluted hydrogen fluoride (HF) etchant (HF 0.5, 1, 5, and 10%) solutions, the concentrations of which were carefully determined via preliminary experiments in order to regulate the surface etching process.

In this study, the type of glass texturing pattern was changed by using the HF-based solutions to vary the etching conditions; the three different types of glass texturing patterns fabricated in this study are respectively illustrated as Etch-1, Etch-2, and Etch-3 in Fig. 1(b). The optimum etching conditions for each textured glass structure and HF solution were obtained following analysis of the results of multiple etching experiments (Before etching of glass: ~700 μm, and after etching of glass: ~696 μm). The scanning electron microscope (SEM) images of each textured surface are presented in Table 1 according to the etching conditions. Fig. 1(c) shows the layered structure of the HIT silicon solar cell to which the textured glass substrate was applied. A commercial n-type solar-grade Si wafer (1.5 Ω·cm, 160 μm thickness, (100) oriented) was used as the base material. Standard RCA techniques (RCA-1: H<sub>2</sub>O<sub>2</sub>-NH<sub>4</sub>OH-H<sub>2</sub>O and RCA-2: H<sub>2</sub>O<sub>2</sub>-HCl-H<sub>2</sub>O) were employed to clean the wafer after ultrasonic treatment; the base wafers were then dipped into diluted HF 1% solution before being placed in the vacuum chamber. Very thin a-Si:H layers were deposited at a temperature of 200°C via chemical vapor deposition by using a gas source comprising SiH<sub>4</sub>, H<sub>2</sub>, B<sub>2</sub>H<sub>6</sub>, and PH<sub>3</sub>; the details of this deposition technique have been provided in a previous report<sup>18</sup>). Ag and Al electrodes were installed on the indium thin oxide film at the front of the cell, and the metal electrodes were installed on a zinc-oxide transparent conducting oxide (TCO) film on the opposite side; a screen-printing technique that has been proven to yield good ohmic contact resistance was used to fabricate the

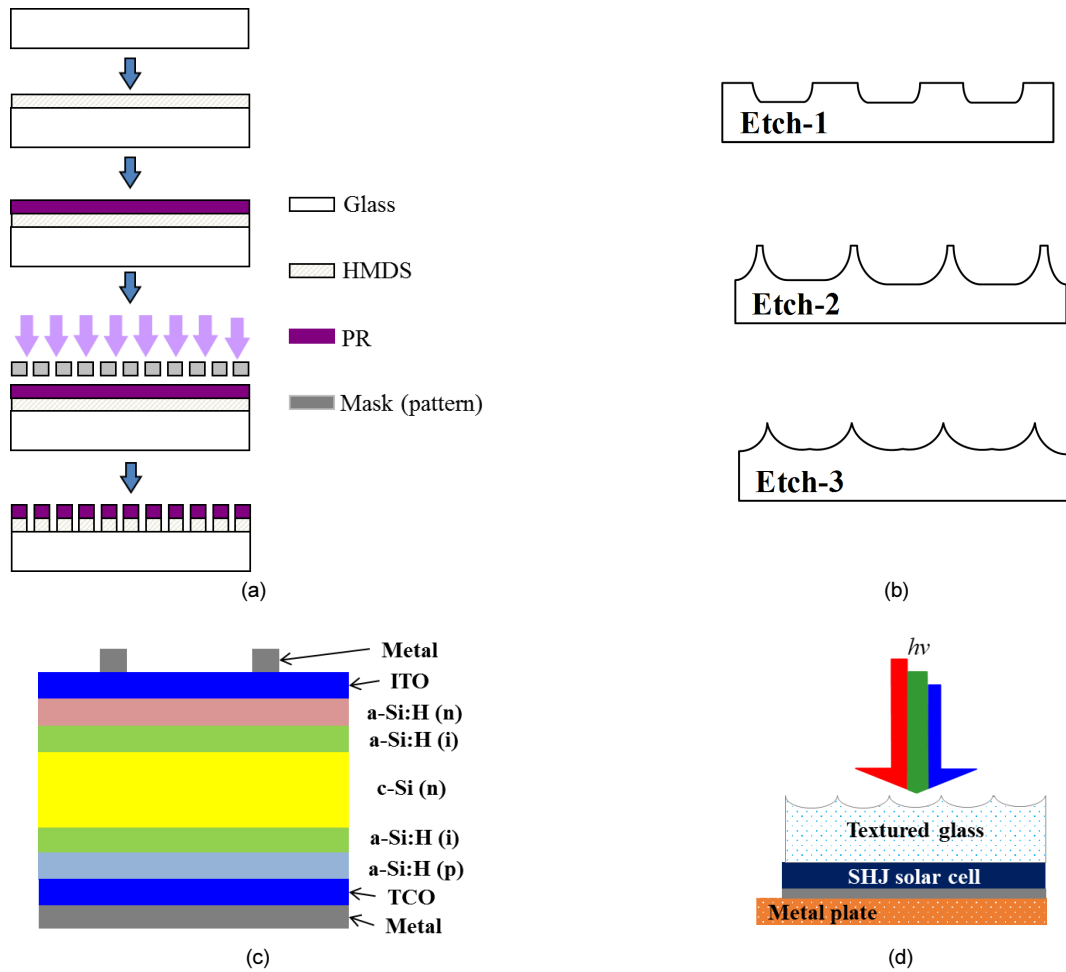


**Fig. 1.** (a) Ultraviolet photolithography process for cover glass texturing, (b) types of textured glasses, (c) layers of HIT Si solar cell, and (d) module structure including the textured cover glass and HIT Si solar cells

**Table 1.** Glass texturing structures according to chemical etching conditions, and structural parameters (aspect ratio) and haze values ( $H_T$ )

Structure	Etching solution	Etch rate ( $\mu\text{m}/\text{min}$ )	Etch depth ( $\mu\text{m}$ )	$H_T$ (%)	Aspect ratio	
	Etch-1	HF 0.5%	0.05	0.59	46	0.17
		HF 1%	0.12	0.63	48	0.19
		HF 5%	0.61	0.67	39	0.23
		HF 10%	1.16	0.61	54	0.17
	Etch-2	HF 0.5%	0.05	1.93	65	0.41
		HF 1%	0.12	1.94	67	0.43
		HF 5%	0.61	1.97	65	0.47
		HF 10%	1.16	1.81	72	0.37
	Etch-3	HF 0.5%	0.05	1.39	52	0.22
		HF 1%	0.12	1.43	83	0.27
		HF 5%	0.61	1.45	79	0.28
		HF 10%	1.16	1.36	63	0.2

metal electrodes. The textured cover glasses were applied over the top layer of the mini-PV module of the fabricated HIT Si solar cells, as is shown in Fig. 1(d).

The total and diffuse transmittance of the textured glasses were measured by using an integrating sphere of a quantum efficiency (QE) instrument (Model: QEX10, PV Measurements

Inc.), and the haze ratio was defined as the ratio of the diffuse transmittance to total transmittance. We analyzed a cross-sectional view of the textured glass surface by using a focused ion beam (Model: LYRA3, TESCAN). The performance of the mini-PV module was characterized by carrying out current density-voltage (J-V) measurements under illumination (AM 1.5 and 100 mW/cm<sup>2</sup>) at room temperature (25°C). The QE of the PV module was characterized by using a QEX10 solar cell measurement system to measure the spectral response, QE, and incident photon to current efficiency.

### 3. Results and Discussion

The ability to perform light scattering is an important attribute that PV module covering glass should possess, and it can be quantitatively assessed by determining the haze value. Because haze is also related to the aspect ratio and structural angle of the periodic textured glass structure, it can be controlled by varying the etch rate and HF solution concentration, as is presented in Table 1<sup>19,20</sup>. In this study, we defined the structural angle as the measured average oblique angle of the textured glass structure, and the aspect ratio as the height divided by the width of the textured structure. Fig. 2 shows that structural angle tends to increase as the aspect ratio increases, and that the over-etched structure of Etch-3 yields a smaller aspect ratio and structure angle than the moderately etched structure of Etch-2. The largest structural angle (57°) was measured from the Etch-2 structure, which also yielded a high aspect ratio of 0.5 relative to aspect ratios determined from Etch-1 structures with structural angles within the range of 31–34°. Note that the structural angle can be observed to increase in coincidence with the aspect ratio, indicating that the AR effect was able to trap incoming light; this phenomenon is due to a higher RMS roughness and, consequently, a higher current density<sup>21</sup>.

We investigated the light scattering characteristics of PV module cover glass with periodic texturing patterns; the results are shown in Fig. 3. Park *et al.* and other research groups reported that light scattering behaviors were enhanced by applying periodic texturing patterns, which thus results in highly efficient Si-based thin film solar cells<sup>22-26</sup>. Similarly, we simulated the light scattering behavior on three types of textured glasses (Etch-1, Etch-2, and Etch-3) by using a finite-difference time-domain (FDTD) simulation method, which is a numerical analysis method commonly used to model computational electrodynamics. For practical comparison, we chose to simulate

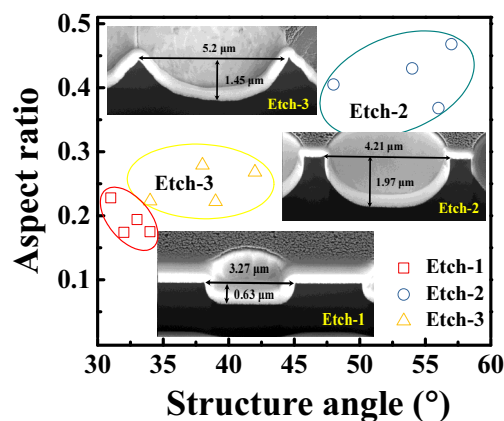
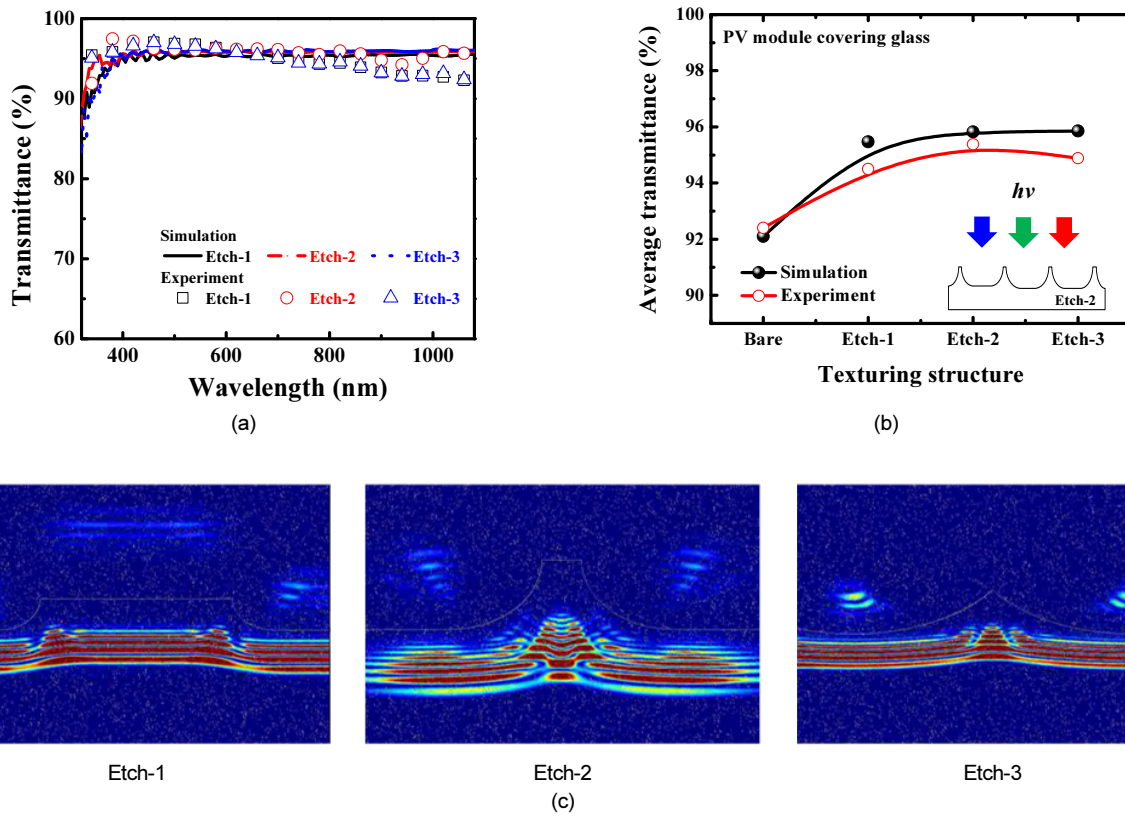


Fig. 2. Aspect ratio as a function of structural angle for the various types of textured PV mini-module cover glass (Etch-1, Etch-2, and Etch-3)

the textured structure for each type as based on the best aspect ratio; thus, the structures with aspect ratios of 0.23, 0.47, and 0.28 were used to represent Etch-1, Etch-2, and Etch-3, respectively.

Fig. 3(a) shows the simulated and measured spectral transmittance of the textured glasses; it can be seen that all textured glasses have good transmittance; particularly, in simulation, the textured glasses were found to exhibit high transmittance (over 95%) for a spectral range of 400–1100 nm. This is because the textured surfaces can effectively suppress the reflectance on the front surface; the small discrepancy with the measured values is due to the reflection from the rear flat surfaces of the glasses. In Fig. 3(b), it can be seen that the simulated and measured average transmittance values are in good agreement; the average transmittance and reflectance of all textured glasses were approximately 95.8% and 4.2%, respectively; these results are better than those for bare glass, which has a transmittance and reflectance of 92.1% and 7.9%, respectively. The reduced reflectance was visualized via FDTD simulation, and the images of demonstrating how light waves propagate immediately after reaching the selected textured structures (Etch-1, Etch-2, and Etch-3) are presented in Fig. 3(c). In the cases of Etch-1 and Etch-3, the surface reflectance was higher than that of Etch-2. The reason for this is that the notch of the Etch-2 glass collects the incident light wave and causes the incoming light wave to diffuse before reflection. These results imply that the Etch-2 textured glass is more suitable for implementation as AR front glass than Etch-1 and Etch-3<sup>27</sup>.

Using the cover glasses with the texture structures detailed in Table 1, we assembled PV modules with HIT Si solar cells and measured their performance parameters, which are listed in



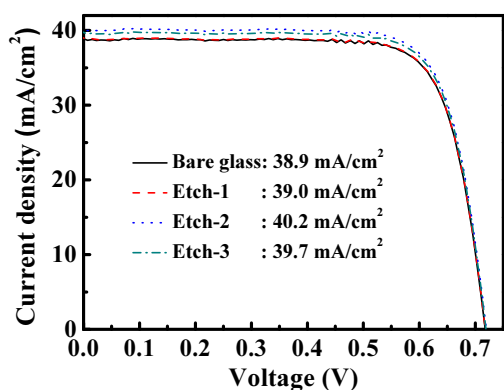
**Fig. 3.** FDTD simulation and measurement results for Etch-1, Etch-2, and Etch-3. (a) Spectral transmittance and (b) average transmittance for the wavelength range of 400 to 1100 nm, and (c) FDTD simulation images of the light wave propagation occurring immediately after light reaches the textured surface

**Table 2.** Comparison of I-V and structural results of PV modules with different texturing glass

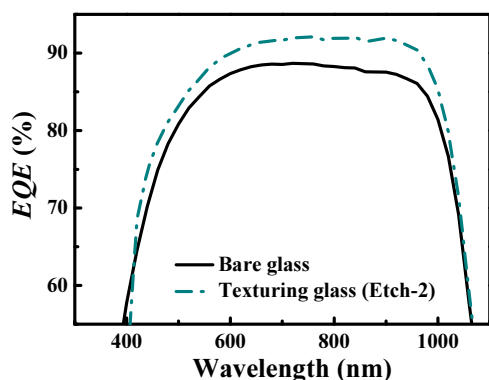
Structure	Etching solution	$V_{oc}$ (mV)	$J_{sc}$ (mA/cm <sup>2</sup> )	FF (%)	$\eta$ (%)
Bare glass		726.3	38.9	76.62	21.65
Etch-1	HF 0.5%	723.4	38.5	76.96	21.43
	HF 1%	722.1	38.84	76.3	21.4
	HF 5%	725.8	39	76.73	21.72
	HF 10%	724.7	38.9	76.35	21.52
Etch-2	HF 0.5%	721.9	39.67	76.47	21.9
	HF 1%	726	39.81	76.65	22.15
	HF 5%	727.5	40.2	76.62	22.41
	HF 10%	726.1	39.58	74.7	21.47
Etch-3	HF 0.5%	725.8	38.86	75.42	21.27
	HF 1%	729.3	39.29	76.23	21.84
	HF 5%	726.8	39.7	76.38	22.04
	HF 10%	731.1	39.42	74.47	21.46

Table 2:  $V_{oc}$ ,  $J_{sc}$ , fill factor (FF), and efficiency ( $\eta$ ). The results presented in Table 2 also indicate that glass with a textured structure can improve module performance. We also measured the current density-voltage ( $J-V$ ) characteristics associated with each of the selected textured structures, i.e., the optimal Etch-1, Etch-2, and Etch-3 structures; the results are illustrated in Fig. 4. Because the highest short-circuit current

density ( $J_{sc}$ ) value for Etch-2 was 40.2 mA/cm<sup>2</sup>, which is higher than that for the non-textured-glass module (38.9 mA/cm<sup>2</sup>), the PV module with the Etch-2 textured cover glass structure was selected for comparison with the non-textured cover glass module. The external quantum efficiency (EQE) results are illustrated in Fig. 5 as a function of wavelength. As was expected, for the wavelength range of 400 to 1100 nm, the PV



**Fig. 4.** Comparison of current density as a function of applied voltage ( $I$ - $V$  curves) for PV modules with a non-textured cover glass and Etch-1-, Etch-2-, and Etch-3-type cover glasses



**Fig. 5.** EQE curves for PV modules with a non-textured cover glass and an Etch-2-type textured cover glass

module with textured cover glass yielded a more desirable EQE response than that with non-textured cover glass; this superior EQE response consequently significantly increases the  $J_{SC}$ . This relatively increased  $J_{SC}$  is due to the fact that the increased aspect ratio and structural angle of textured cover glass promotes sufficient light scattering and low reflectivity.

## 4. Conclusion

We developed and evaluated glass texturing patterns that can be applied to the cover glass of HIT Si solar cell PV modules. Periodic honeycomb textures were formed on the PR-patterned glass surface by using HF solutions. The HF solutions and corresponding optimal etching conditions were varied to develop three different types of textured structures. Analysis of the textured structures revealed that the texturing parameters can be controlled over wide ranges of structural angle ( $31$ – $57^\circ$ ) and aspect ratio ( $0.17$ – $0.47$ ). Moreover, by evaluating the haze ratio and spectral transmittance of each textured structure, we

optimized the texturing parameters for each type of textured structure. FDTD simulations were also performed, the results of which demonstrated that the transmittance increased for all textured glasses because the reflectance was suppressed on the textured surface, and that Etch-2 most effectively reduced the surface reflectance. The various textured structures developed in this study were applied to the cover glass of PV modules with HIT Si solar cells. Texturing the surfaces of cover glasses was also found to increase the  $J_{SC}$  of the PV module, with the Etch-2 structure yielding the highest  $J_{SC}$  value of  $40.2 \text{ mA/cm}^2$ . Our approach can be applied to various PV modules, not only for high-performance HIT Si solar cells, but also for conventional crystalline Si solar cells; thus, it has the potential to further strengthen the industrial and technical competitiveness of crystalline silicon solar cells.

## Acknowledgment

This work was supported by the Korea Institute of Energy Technology Evaluation and Planning (KETEP) and the Ministry of Trade, Industry & Energy (MOTIE) of the Republic of Korea (No. 20153030012590).

## References

1. K. Yoshikawa, H. Kawasaki, W. Yoshida, T. Irie, K. Konishi, K. Nakano, T. Uto, D. Adachi, M. Kanematsu, H. Uzu, J. Yamamoto, "Silicon heterojunction solar cell with interdigitated back contacts for a photoconversion efficiency over 26%", *Nat. Energy*, Vol. 2, 17032, 2017.
2. C. Battaglia, A. Cuevas, S. De Wolf, "High-efficiency crystalline silicon solar cells: status and perspectives", *Energy Environ. Sci.*, Vol. 9, pp. 1552-1576, 2016.
3. F. Mavromatakis, F. Vignola, B. Marion, "Low irradiance losses of photovoltaic modules", *Sol. Energy*, Vol. 157, pp. 496-506, 2017.
4. P. G. Piedra, L. R. Llanza, H. Moosmüller, "Optical losses of photovoltaic modules due to mineral dust deposition: Experimental measurements and theoretical modeling", *Sol. Energy*, Vol. 164, pp. 160-173, 2018.
5. B. Geetha Priyadarshini, A. K. Sharma, "Design of multi-layer anti-reflection coating for terrestrial solar panel glass", *Bull. Mater. Sci.*, Vol. 39, No. 3, pp. 683-689, 2016.
6. D. Huh, J.-H. Shin, M. Byun, S. Son, P.-H. Jung, H.-J. Choi, Y.-D. Kim, H. Lee, "Analysis of long-term monitoring data of PV module with SiO<sub>x</sub>-based anti-reflective patterned protective glass", *Sol. Energy Mater. Sol. Cells*, Vol. 170, pp. 33-38, 2017.
7. R. Bohme, K. Zimmer, "Low roughness laser etching of fused

- silica using an adsorbed layer”, *Appl. Surf. Sci.*, Vol. 239, pp. 109-116, 2004.
8. F. Chen, H. Liu, Q. Yang, X. Wang, C. Hou, H. Bian, W. Liang, J. Si, X. Hou, “Maskless fabrication of concave microlens arrays on silica glasses by a femtosecond-laser-enhanced local wet etching method”, *Opt. Express*, Vol. 18, No. 19, pp. 20334-20343, 2010.
  9. C. Xie, X. Li, K. Liu, M. Zhu, R. Qiu, Q. Zhou, “Direct writing of sub-wavelength ripples on silicon using femtosecond laser at high repetition rate”, *Appl. Surf. Sci.*, Vol. 360, pp. 896-903, 2016.
  10. C. Battaglia, C. M. Hsu, K. Söderström, J. Escarre, C. Ballif, “Light trapping in solar cells: can periodic beat random?”, *ACS Nano*, Vol. 6, No. 3, pp. 2790-2797, 2012.
  11. P. Spinelli, V. E. Ferry, J. V. D. Groep, M. V. Lare, A. Polman, “A Plasmonic Light Trapping in Thin-Film Si Solar Cells”, *J. Opt.*, Vol. 14, No. 2, pp. 024002-024013, 2012.
  12. G. Kumaravelu, M. M. Alkaisi, A. Bittar, D. Macdonald, J. Zhao, “Damage studies in dry etched textured silicon surfaces”, *Current. Appl. Phys.*, Vol. 4, No. 2-4, pp. 108-110, 2004.
  13. M. Tucci, E. Salurso, F. Roca, F. Palma, “Dry cleaning process of crystalline silicon surface in a-Si:H/c-Si heterojunction for photovoltaic applications”, *Thin Solid Films*, Vol. 403-404, pp. 307-311, 2002.
  14. J. Yoo, K. Kim, M. Thamilselvan, N. Lakshminarayan, Y. K. Kim, J. H. Lee, K. J. Yoo, J. Yi, “RIE texturing optimization for thin c-Si solar cells in SF<sub>6</sub>/O<sub>2</sub> plasma”, *J. Phys. D: Appl. Phys.*, Vol. 41, No. 12, 125205, 2008.
  15. A. Hongsingthong, T. Krajangsang, I. A. Yunaz, S. Miyajima, M. Konagai, “ZnO Films with Very High Haze Value for Use as Front Transparent Conductive Oxide Films in Thin-Film Silicon Solar Cells”, *Appl. Phys. Express*, Vol. 3, pp. 051102-051111, 2010.
  16. A. Hongsingthong, I. A. Yunaz, S. Miyajima, M. Konagai, “Preparation of ZnO thin films using MOCVD technique with D<sub>2</sub>O/H<sub>2</sub>O gas mixture for use as TCO in silicon-based thin film solar cells”, *Sol. Energy Mater. Sol. Cells*, Vol. 95, No. 1, pp. 171-174, 2011.
  17. H. Zhang, B. Ding, T. Chen, “A high efficiency industrial polysilicon solar cell with a honeycomb-like surface fabricated by wet etching using a photoresist mask”, *Appl. Surf. Sci.*, Vol. 387, pp. 1265-1273, 2016.
  18. S. B. Kim, S. M. Iftiqar, D. H. Lee, H. J. Lee, J. H. Kim, J. H. Jung, D. H. Oh, V. A. Dao, J. Yi, “Improvement in Front-Contact Resistance and Interface Passivation of Heterojunction Amorphous/Crystalline Silicon Solar Cell by Hydrogen-Diluted Stack Emitter”, *IEEE J. Photovolt.*, Vol. 6, No. 4, pp. 837-845, 2016.
  19. J. -Y. Li, C. -H. Hung, C. -Y. Chen, “Hybrid black silicon solar cells textured with the interplay of copper-induced galvanic displacement”, *Sci. Rep.*, Vol. 7, pp. 17177, 2017.
  20. L. Chen, Q. Wang, W. Chen, H. Huang, X. Shen, “Investigation of a novel frosted glass with regular pit array texture”, *J. Mat. Proc. Techno.*, Vol. 238, pp. 195-201, 2016.
  21. T. Maier, D. Bach, P. Müllner, R. Hainberger, H. Brückl, “Antireflective surface structures in glass by self-assembly of SiO<sub>2</sub> nano particles and wet etching”, *Opt. Express*, Vol. 21, No. 17, 20254, 2013.
  22. H. S. Park, M. H. Shin, H. S. Kim, S. B. Kim, A. H. Tuan Le, J. Y. Kang, Y. J. Kim, D. P. Pham, J. H. Jung, J. Yi, “Investigation of 3-dimensional structural morphology for enhancing light trapping with control of surface haze”, *Opt. Mater.*, Vol. 66, pp. 404-409, 2017.
  23. S. Q. Hussain A. H. Tuan Le, K. Mallem, H. S. Park, M. K. Ju, Y. J. Kim, J. H. Cho, J. J. Park, Y. K. Kim, J. Yi, “Using the light scattering properties of multi-textured AZO films on inverted hemisphere textured glass surface morphologies to improve the efficiency of silicon thin film solar cells”, *Appl. Surf. Sci.*, Vol. 447, pp. 866-875, 2018.
  24. H. S. Park, S.-H. Nam, M. H. Shin, M. K. Ju, Y.-J. Lee, J.-H. Yu, J. H. Jung, S. B. Kim, S. H. Ahn, J.-H. Boo, J. Yi, “Method for Fabricating Textured High-Haze ZnO:Al Transparent Conduction Oxide Films on Chemically Etched Glass Substrates”, *J. Nanosci. Nanotechnol.* Vol. 16, No. 5, pp. 4886-4892, 2016.
  25. H. S. Park, M. H. Shin, H. S. Kim, S. B. Kim, A. H. Tuan Le, Y. K. Kim, S. H. Ahn, J.-J. Jeong, J. Yi, “Wideband Light Scattering of Periodic Micro Textured Glass Substrates for Silicon Thin-Film Solar Cells”, *J. Nanosci. Nanotechnol.*, Vol. 17, No. 11, pp. 8562-8566, 2017.
  26. H. S. Park, Y. -J. Lee, S. H. Ahn, S. B. Kim, J. Yi, “Effect of wet textured glass surface morphology on the haze ratio and aspect ratio for amorphous silicon thin film solar cells”, *J. Renew. Sustain. Energy*, Vol. 6, No. 5, 053141, 2014.
  27. S. M. Ji, K. J. Song, T. B. Nguyen, N. S. Kim, H. Lim, “Optimal Moth Eye Nanostructure Array on Transparent Glass Towards Broadband Antireflection”, *ACS Appl. Mater. Interfaces*, Vol. 5, No. 21, pp. 10731-10737, 2013.